Received: 7 May 2020 | Accepted: 12 October 2020

DOI: 10.1111/jth.15142

ORIGINAL ARTICLE

jth

Blocking von Willebrand factor free thiols inhibits binding to collagen under high and pathological shear stress

Harrison E. R. O'Brien[1,2] | X. Frank Zhang[3,4] | Maximo Sanz-Hernandez[5] | Alain Chion[6] | Susan Shapiro[7,8] | Golzar Mobayen[1] | Yan Xu[3,4] | Alfonso De Simone[5] | Michael A. Laffan[1] | Thomas A. J. McKinnon[1]

[1]Department of Immunology and Inflammation, Centre for Haematology, Imperial College of Science Technology and Medicine, London, UK

[2]Institute of Structural and Molecular Biology, University College London, London, UK

[3]Department of Bioengineering, Department of Mechanical Engineering and Mechanics, Lehigh University, Bethlehem, PA, USA

[4]Department of Mechanical Engineering and Mechanics, Lehigh University, Bethlehem, PA, USA

[5]Department of Life Sciences, Imperial College London, London, UK

[6]Irish Centre for Vascular Biology, Molecular and Cellular Therapeutics, Royal College of Surgeons in Ireland, Dublin, Ireland

[7]Oxford University Hospitals NHS Foundation Trust, Oxford NIHR Biomedical Research Centre, Oxford, UK

[8]Radcliffe Department of Medicine, Oxford University, Oxford, UK

Correspondence
Thomas A. J. McKinnon, Department of Immunology and Inflammation, Centre for Haematology, Imperial College London, 5th Floor, Commonwealth Building, Hammersmith Hospital Campus, Du Cane Road, London W12 0NN, UK.
Email: t.mckinnon03@imperial.ac.uk

Funding information
British Heart Foundation, Grant/Award Number: FS/11/3/28632; Heart Foundation, Grant/Award Number: 11, 3 and 28632

Abstract

Background: Von Willebrand factor (VWF) contains a number of free thiols, the majority of which are located in its C-domains, and these have been shown to alter VWF function, However, the impact of free thiols on function following acute exposure of VWF to collagen under high and pathological shear stress has not been determined.

Methods: VWF free thiols were blocked with N-ethylmaleimide and flow assays performed under high and pathological shear rates to determine the impact on platelet capture and collagen binding function. Atomic force microscopy (AFM) was used to probe the interaction of VWF with collagen and molecular simulations conducted to determine the effect of free thiols on the flexibility of the VWF-C4 domain.

Results: Blockade of VWF free thiols reduced VWF-mediated platelet capture to collagen in a shear-dependent manner, with platelet capture virtually abolished above 5000 s^{-1} and in regions of stenosis in microfluidic channels. Direct visualization of VWF fibers formed under extreme pathological shear rates and analysis of collagen-bound VWF attributed the effect to altered binding of VWF to collagen. AFM measurements showed that thiol-blockade reduced the lifetime and strength of the VWF-collagen bond. Pulling simulations of the VWF-C4 domain demonstrated that with one or two reduced disulphide bonds the C4 domain has increased flexibility and the propensity to undergo free-thiol exchange.

Conclusions: We conclude that free thiols in the C-domains of VWF enhance the flexibility of the molecule and enable it to withstand high shear forces following collagen binding, demonstrating a previously unrecognized role for VWF free thiols.

KEYWORDS

collagen, shear stress, thiols, thrombosis, von Willebrand factor

X. Frank Zhang and Maximo Sanz-Hernandez contributed equally to this work.

Manuscript handled by: X. Long Zheng

Final decision: X. Long Zheng and 12-Oct-2020

1 | INTRODUCTION

Von Willebrand factor (VWF) is a large multimeric plasma glycoprotein essential to normal hemostasis. First, VWF mediates platelet capture to the damaged vessel wall under high shear stress conditions and, second, it is the carrier molecule for factor VIII (Figure 1).[1,2]

Compared with other mammalian proteins, VWF has a uniquely high cysteine content.[3] It was previously understood that all the cysteine residues present in VWF took part in inter- or intra-molecular disulphide bonds.[4-7] However, several recent studies have demonstrated that each VWF molecule contains a number of unpaired cysteine residues or free thiols.[8-11] The majority of these free thiols are located in the C-domains of VWF and have been suggested to impact significantly on VWF function. For example, shearing of VWF in a plate and cone viscometer at high shear stress was shown to enhance VWF platelet binding, but reduced the free thiol content.[8] When sheared in the presence of the thiol-blocking agent N-ethylmaleimide (NEM), platelet capture function was lost, suggesting a crucial role for free thiols in mediating VWF function.[8] Furthermore, it was demonstrated that when soluble VWF was perfused over stimulated human umbilical vein endothelial cells, formation of the VWF string network was blocked by the addition of NEM indicating a role for VWF thiols in the association of soluble VWF with endothelial cell anchored VWF.[11] Subsequently, Ganderton et al[9] reported that VWF lateral self-association involved the Cys2431 and Cys2453 residues in the C3 domain, hypothesizing that disulfide exchange between VWF molecules could occur; however, this was not shown in full-length VWF or under shear stress. Moreover, we previously demonstrated that mutation of the predicted unpaired cysteine residues abolished secretion of VWF, suggesting that proper disulphide bond formation within the endoplasmic reticulum is essential for VWF production.[10] It is therefore unclear how and when certain disulfide bonds are broken or for what purpose. Interestingly, it is now known that the C-terminal domains of sequential VWF monomers form a stem structure.[12,13] Formation of the stem is controlled by pH and calcium-dependent interactions between D4 domains, with the D4 domain thought to act as a force sensor enabling the molecule to elongate in response to changes in shear stress.[14,15] Because the majority of the free thiols are present in the adjacent C-domains that form the VWF stem, it is conceivable that they also play a role in mediating stem formation.

Essentials

- Von Willebrand factor contains a number of free-thiols.
- We investigated how blocking these free-thiols impacts on VWF function under high shear stress.
- Blockade of VWF thiols ablated collagen binding at pathological shear rates.
- VWF free thiols are a novel regulator of collagen binding.

Although blocking VWF free thiols impacts VWF function, these previous studies have not addressed their effects on VWF binding to collagen under shear stress where the protein will be exposed to collagen for a few milliseconds or extremely pathological shear rates such as those found in arterial stenosis where wall shear rates can exceed 100 000 s^{-1}.[16-18] In the present study, we have investigated the role of free thiols in VWF using a physiological system in which the key measure is the ability of VWF to mediate platelet capture to collagen under flow.[19] Our data demonstrate that under conditions of high pathological shear stress, the free thiols in the C-domains of VWF play an unexpected role in promoting collagen binding and subsequent platelet capture.

2 | MATERIAL AND METHODS

2.1 | Materials

3-N-maleimidylpropionyl biotin (MPB), NEM, 3,3′ dihexyloxacarbocyanine iodide (DiOC6), 7K MWCO Zeba-Spin desalting columns were purchased from Thermo Fisher Scientific. Human collagen type III was from Southern Biosciences, collagen type I was purchased from Chronopar and Sigma. Alexa Fluor 488 sulfodichlorophenol ester was purchased from Invitrogen.

2.2 | Purification, labelling and characterization of VWF

Plasma derived VWF was isolated from Voncento (CSL Behring) using gel filtration through a Sephacryl-400 gel filtration column,

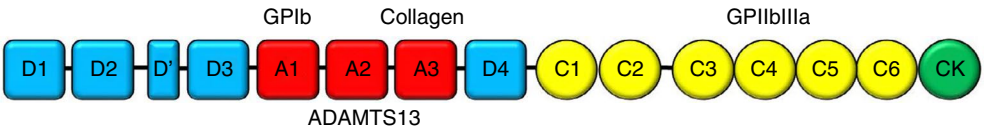

FIGURE 1 Domain organization of VWF. Each full-length VWF monomer comprises a series of repeating domains arranged as depicted. The cysteine knot domain (CK) contains the dimerization site, whereas multimers are formed through disulphide bonding between adjacent D′ and D3 domains and this process requires the propeptide (D1D2 domains). The A1 domain contains the binding site for glycoprotein Ibα, whereas the A2 domain contains the ADAMTS13 cleavage site and the major collagen binding site is located within the A3 domain. The C4 domain contains an RGD sequence that binds to glycoprotein IIbIIIa. The majority of the free thiols that occur in VWF have been previously mapped to the C domains. A monomeric VWF protein spanning the D′ to A3 domains is used in this study and thus lacks the D4 and C domains

as previously described.[20] The first eluted fractions containing purified VWF were quantified by VWF ELISA.[20] Free thiols in VWF were blocked with NEM. A stock solution of 1 mol/L NEM was prepared immediately before use and added to purified VWF, using 10 mM NEM per 100 μg/mL of VWF. Labelling was performed for 30 minutes in the dark at room temperature, then excess NEM removed using Zeba spin desalting columns (ThermoFisher UK) (7K MWCO) and VWF was requantified by ELISA. Typically, >90% of VWF was recovered. Control VWF was treated with buffer and spun through a Zeba spin column in the same way. The D′A3 fragment of VWF was expressed and purified as previously described[21] and treated with NEM in a similar way. Labelling of control and NEM-VWF with Alexa Fluor 488 sulfodichlorophenol ester (AF488) was performed essentially as previously described.[22] In brief, aliquots of control and NEM-VWF in phosphate buffed saline at a concentration of 500 μg/mL in a volume of 500 μL were labelled. In accordance with manufacturer's instructions, 50 μL of a 1 mol/L sodium bicarbonate pH 8.3 solution was added to the samples and AF488 was dissolved in 500 μL dimethylsulfoxide. Ten microliters of AF488 was then added to the VWF and incubated for 60 minutes at room temperature in the dark. Excess AF488 was removed by subsequent passage through a Zebra spin desalting column as described previously and VWF requantified by ELISA. Typically, after AF488 labelling, the recovered VWF yield was >80% with no loss of multimers. Analysis of VWF binding to collagen, GPIbα, GPIIbIIIa, and VWF multimer analysis and incorporation of MPB were all performed essentially as previously described.[21,23]

2.3 | VWF-mediated platelet capture to collagen

Assessment of VWF-mediated platelet capture was performed essentially as described.[21] In brief, Ibidi VI$^{0.1}$ flow chambers or custom-made flow channels generated as previously described[24] were coated with 100 μg/mL human type III collagen (Southern Biosciences) or 200 μg/mL type I collagen (ChronoPar). Plasma free blood (washed platelets and erythrocytes) was prepared using previously described methods. Plasma free blood was supplemented with 5 μg/mL VWF and perfused through the channels at flow rates to give defined wall shear rates. Flow slides were mounted on an epifluorescent microscope (CKX41; Olympus), and real-time recordings were captured via a Rollera XR camera (QImaging) and StreamPix6 4 software. Video images were analyzed offline using freely available Virtual Dub (http://www.virtualdub.org/) and MacBiophotonics ImageJ software (National Institutes of Health).

2.4 | Direct binding of VWF to collagen under shear

Flow channels coated with collagen were perfused with 10 μg/mL VWF in 20 mmol/L Tris-HCl, pH 7.4 at designated shear rates. Following perfusion, the channels were washed with 20 mmol/L Tris-HCl, pH 7.4 by perfusion for 1 minute. Bound protein was stripped by the addition of 2% sodium dodecylsulfate to the channels and heating the slide at 60°C on a heating block for 30 minutes. Stripped samples were then analyzed by VWF ELISA.

2.5 | Atomic force microscopy

For the atomic force microscopy (AFM) studies, human type I collagen at 1 mg/mL (Sigma-Aldrich) was diluted to a final concentration of 0.1 mg/mL in phosphate buffered saline and was covalently attached to an AFM cantilever (MLCT: Bruker Nano) via an established crosslinking protocol using a heterobifunctional PEG linker. [25] Con-VWF or NEM-VWF was also attached to the silanized glass coverslips (Nanocs) using the same protocol. The AFM force measurements were performed on an apparatus designed for operation in the force spectroscopy mode.[26-28] Using a piezoelectric translator, the collagen-functionalized cantilever was lowered onto the glass coverslip with the attached VWF sample until binding between the collagen and the VWF sample occurred. The binding interaction was then determined from the deflection of the cantilever via a position-sensitive two-segment photodiode. To calibrate the cantilever (320 μm long × 22 μm wide triangle), the spring constant at the tip was characterized via thermally induced fluctuations. The spring constants (13 ± 3 pN/nm) of the calibrated cantilevers agreed with the values specified by the manufacturer. Except for the adhesion specificity test, the contact time and indentation force between the cantilever and the sample were minimized to obtain measurements of the unitary VWF-collagen unbinding force. An adhesion frequency of ~30% in the force measurements ensured that there was a >83% probability that the adhesion event was mediated by a single VWF-collagen bond. AFM measurements were collected at cantilever retraction speeds ranging from 0.4 to 10 μm/s to achieve the desired loading rate (~400-10 000 pN/s). All measurements were conducted at 25°C in TBS buffer.

2.6 | Molecular dynamics

The starting structure of the VWF C4 domain (PDB code 6FWN) was energy minimized and solvated in Tip3p waters, using a dodecahedron box of dimensions 12.9 nm × 6.9 nm × 6.9 nm.[29] The charge of the system was kept neutral by addition of four sodium ions. All simulations were performed in the NPT ensemble, with a timestep of 2 fs. Temperature was coupled using the V-rescale method[30] (300 K, with coupling constant of 0.1 ps), and pressure used the Berendsen algorithm (reference pressure of 1 bar, coupling constant of 1 ps).[31] We used periodic boundary conditions and the LINCS algorithm for constraints.[32] Electrostatic interactions were accounted for by the Particle-mesh Ewald method.[33] All simulations used the force field AMBER99SB-ILDN.[34] Initially every form of the

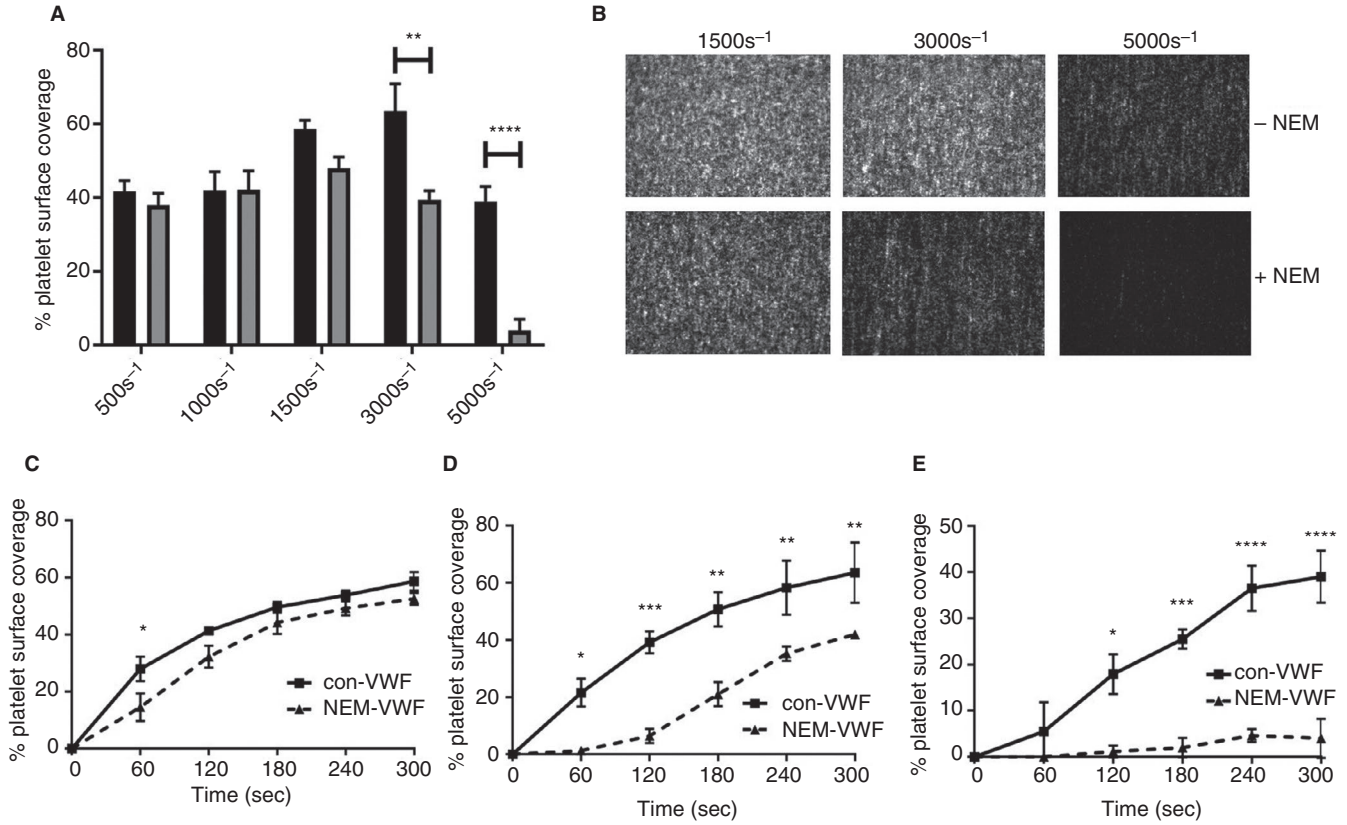

FIGURE 2 Blocking VWF free thiols with NEM reduces VWF-mediated platelets capture to collagen in a shear-dependent manner. Ibidi VI$^{0.1}$ flow slides coated with 100 μg/mL human type III collagen were perfused with plasma free blood supplemented with control or NEM-treated VWF at indicated shear rates. Platelets were rendered fluorescent with DiOC6 and platelet surface coverage was monitored in real-time. A, Platelet surface coverage after 5 min perfusion at 500 s^{-1} to 5000 s^{-1} for control VWF (black bars) and NEM-VWF (gray bars). Data are mean ± SD (n = 4). B, Real-time images captured after 5 min perfusion at 1500, 3000, and 5000 s^{-1}. C-E, Time course of platelet surface coverage between 0 and 300 s at 1500 s^{-1} (C), 3000 s^{-1} (D), and 5000 s^{-1} (E) for control VWF (solid lines) and NEM-VWF (dashed lines). Data are mean ± SD (n = 4). $^{**}P < .005$, $^{***}P < .0005$, $^{****}P < .00005$

VWF C4 domain was pulled by applying opposite forces of 1000 kJ/mol (along the *x*-axis direction) on the N- and C-termini. We then extracted equally spaced structures along this pulling pathway, with a spacing of 0.1 nm. Each of these structures was simulated for 5 ns using a biasing umbrella potential used to later calculate the potential of mean force (PMF).[35] The final energy profiles of the PMF calculation were reconstructed using the weighted histogram analysis method, discarding the first nanosecond of each simulation as an equilibration phase. Finally, the thiol exchange was modelled by replacing one of the disulphide forming residues with the free cysteine, and applying opposite forces to the termini (1000 kJ/mol along the *x*-axis direction) until the maximum extension of the domain was reached. Simulations and analyses were performed with the GROMACS molecular simulations package.[36]

2.7 | Statistical analysis

Statistical analysis was performed using Prism7 software, using either a standard one-way ANOVA with multiple comparisons or Student *t* test.

3 | RESULTS

3.1 | Blockade of free thiols reduces VWF-mediated platelet capture in a shear-dependent manner

To investigate the role of free thiols in VWF-mediated platelet capture, VWF was treated with NEM to block unpaired cysteines. Consistent with previous observations, VWF could incorporate MPB demonstrating the presence of free thiols, and MPB binding was lost following NEM treatment (Figure S1).[8,37] Additionally, NEM labelling did not alter the ability of VWF to interact with collagen, GPIbα, or GPIIbIIIa under static conditions and did not alter its multimeric profile (Figure S1). Subsequently, NEM-labelled VWF was added to plasma free blood and perfused over collagen at a range of shear rates for 5 minutes. After 5 minutes' perfusion at 500 s^{-1} and 1000 s^{-1}, there was no observable difference in the ability of NEM-VWF to mediate platelet capture compared to control VWF at all-time points. When the shear rate was increased to 1500 s^{-1}, NEM-VWF became visibly less able to mediate platelet capture although this failed to reach statistical significance. At 3000 s^{-1}, there was a significant reduction in the ability of NEM-VWF to capture

platelets and at 5000 s^{-1} virtually no platelet capture was observed with NEM-VWF, whereas capture by WT VWF was well maintained (Figure 2A & B). When analyzed over a time course, NEM-VWF demonstrated significantly reduced platelet capture at 60, 120, and 180 seconds at 1500 s^{-1} (Figure 2C) and at 3000 and 5000 s^{-1} platelet capture was significantly reduced at all-time points (Figure 2D,E). These data clearly demonstrate a critical role for VWF free thiols in VWF function, which becomes apparent only under high and pathological shear stress. Because these experiments were performed in the absence of ADAMTS13, perfusion assays were repeated supplementing plasma free blood with both VWF and recombinant ADAMTS13. Consistent with our previously published observations, the addition of ADAMTS13 reduced the extent of VWF-mediated platelet capture.[38] No observable differences were seen in the extent of platelet capture lose with NEM-VWF at 1500 s^{-1} compared with control VWF. With NEM-VWF at 3000 s^{-1}, ADAMTS13 fully abolished platelet capture; however, this reflects the reduced function of NEM-VWF at this shear rate, rather than increased susceptibility to ADAMTS13 proteolysis (Figure S2).

3.2 | Blockade of VWF free thiols reduces platelet capture at stenotic sites

Because blocking VWF free thiols with NEM reduced VWF mediated platelet capture in a shear dependent manner, we hypothesized that at sites of altered shear stress such as stenoses where shear rates can exceed physiological levels, platelet capture would be similarly affected. Microfluidic slides designed to mimic a constricted vessel were coated with collagen and perfused with plasma free blood supplemented with either con- or NEM-VWF and platelet capture recorded at different sections of the channel corresponding to increasing shear rates (Figure 3A). In keeping with the previous results, at regions of physiological shear rates (~1500 s^{-1}) a similar extent of platelet surface coverage was observed. However, as the shear rate increased to ~4000 s^{-1}, there was a marked reduction in platelet capture. At the constricted region of the channel where the wall shear rate was highest (~25 000 s^{-1}), con-VWF mediated the formation of dense platelet rich thrombi; however, no platelet capture was observed with NEM-VWF (Figure 3B).

3.3 | Thiol blockage has minimal effect on VWF binding to collagen under static conditions

Because NEM-VWF demonstrated reduced platelet capture on collagen under shear stress, we determined whether similar observations could be made under static conditions. NEM treatment of VWF did not affect binding to collagen in a static plate assay or alter the multimeric profile (data not shown). To establish if NEM-VWF coated to collagen under static conditions could still capture platelets, collagen-coated flow slides were precoated with con- or NEM-VWF under static conditions or by perfusion of the VWF alone at 3000 or 5000 s^{-1}. Following this, washed platelets and red blood cells were perfused over the static-coated VWF at 3000 or 5000 s^{-1} and over the shear-coated VWF at the same shear as used for coating. Consistent with these observations, when VWF was previously coated under shear stress, there was a shear-dependent decrease in the ability of NEM-VWF to capture platelets (Figure 4). Conversely, NEM-VWF that had been previously coated statically was able to mediate platelet capture at both shear rates (Figure 4). These data show that the impaired platelet capture of

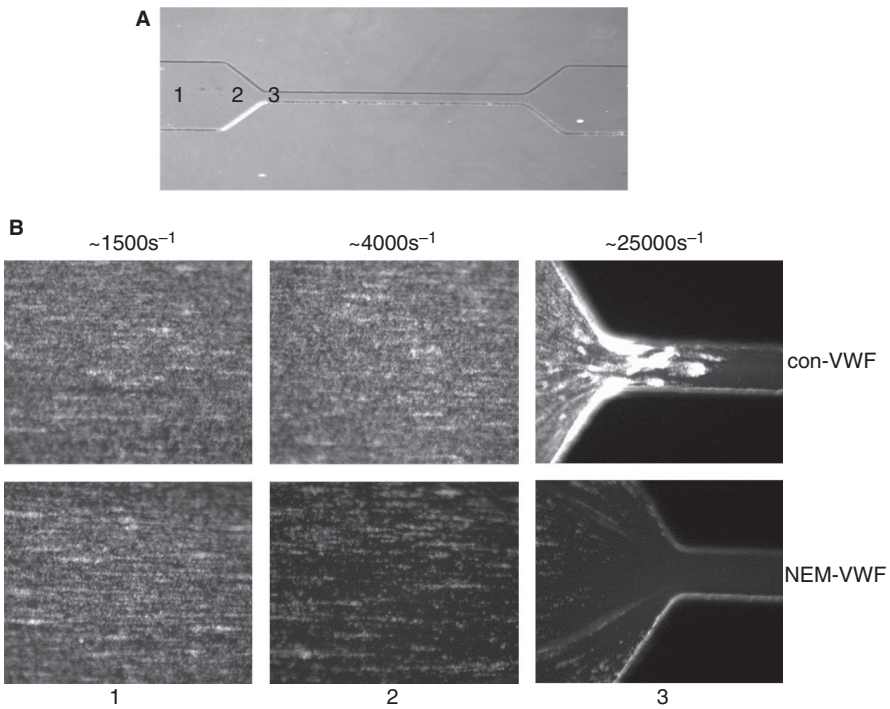

FIGURE 3 Blocking VWF free thiols selectively abolishes platelet capture at stenotic regions under a dynamic shear range. Custom made PDMS flow channels were produced to mimic a stenotic region and coated with collagen type III and perfused with plasma free blood supplemented with control or NEM-treated VWF. A, Light microscope image of the stenotic channel. B, Real-time images of platelet surface coverage taken at three regions from the stenotic channel (as labelled in panel A), with wall shear rates corresponding to ~1500 s^{-1}, ~4000 s^{-1}, and ~25 000s^{-1}. Representative images of four independent experiments

the NEM-VWF results from alteration in its interaction with collagen under shear stress.

3.4 | Free thiols in the C-domains of VWF are required for collagen binding under high shear stress

Because NEM-VWF was able to effectively mediate platelet capture to collagen at 500 to 1500 s^{-1} and when coated to collagen surfaces under static conditions; the effect of blocking VWF free thiols was unlikely to be attributable to altered platelet-VWF binding. To further confirm this, flow slides were coated with VWF-D′A3 protein treated with NEM and then perfused with washed red blood cells and platelets. NEM treatment of the D′A3 fragment did not alter its ability to capture platelets (Figure 5A). Moreover, when the D′A3 was bound to collagen under static conditions, NEM treatment again did not alter platelet capture (Figure 5B), suggesting, first, the observed effects are limited to collagen binding under conditions of flow and, second, suggesting that the C-domains play an important role in mediating this effect. To demonstrate this further, type I collagen surfaces were perfused at 66 000 s^{-1} with VWF-488 and fiber formation recorded in real-time. The labelling of VWF with Alexa Fluor 488 sulfodichlorophenol ester did not alter multimeric content (Figure S3A).

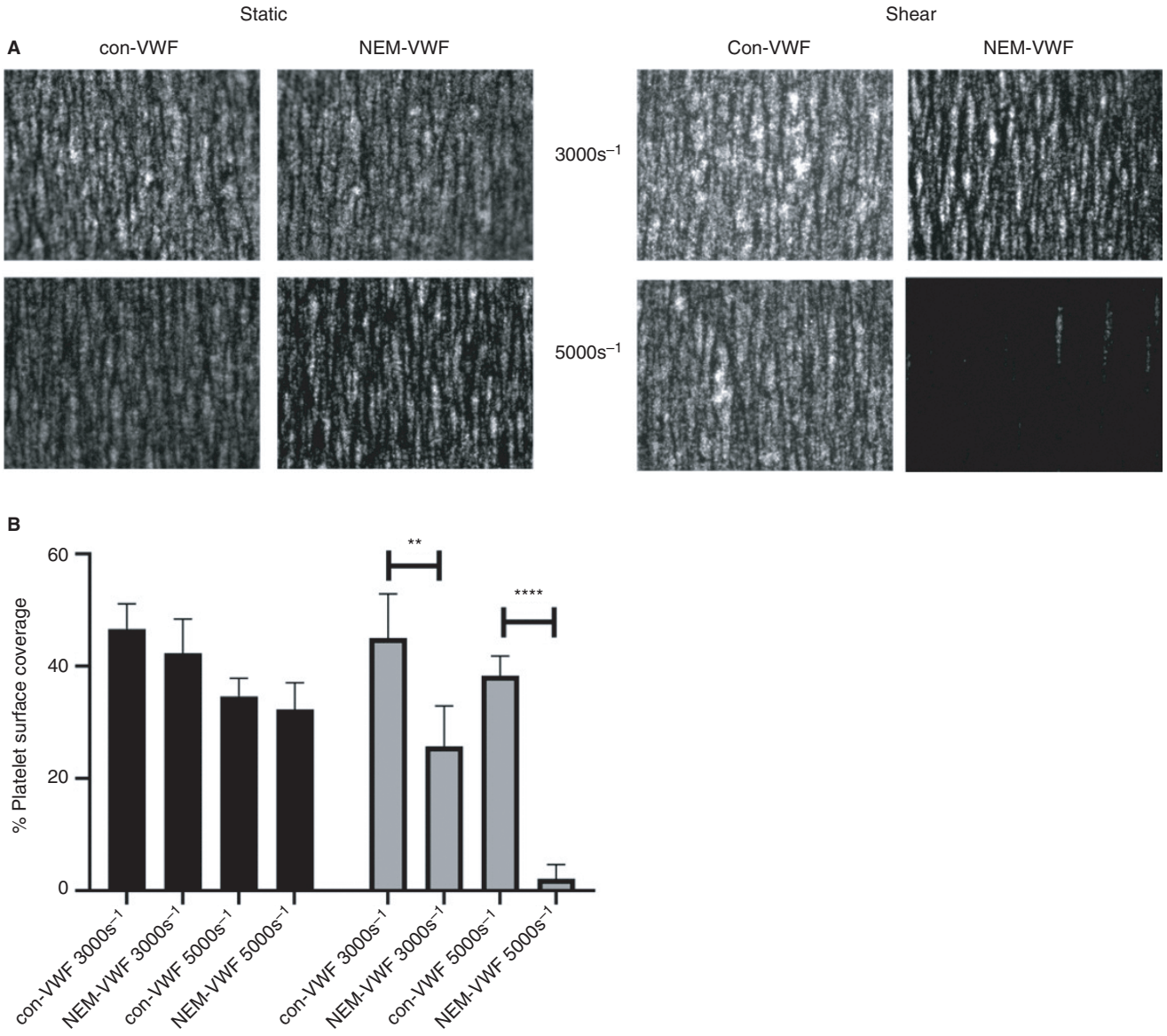

FIGURE 4 Blockade of VWF free thiols has minimal effect on collagen binding under static conditions. Ibidi $VI^{0.1}$ flow slides coated with 100 μg/mL human type III collagen were incubated with 10 μg/mL control or NEM-VWF under static conditions for 60 min at room temperature or perfused with 10 μg/mL control or NEM-VWF diluted in 20 mmol/L Tris, pH 7.4 for 5 min at 3000 or 5000 s^{-1}. Channels were then subsequently perfused with plasma free blood at the stated shear rates and capture of DiOC6-labelled platelets recorded after 5 min perfusion (A). Platelet surface coverage after 5 min was determined using ImageJ (coat static, black bars) (coat-flow, gray bars) (B). Data are mean ± SD (n = 4)

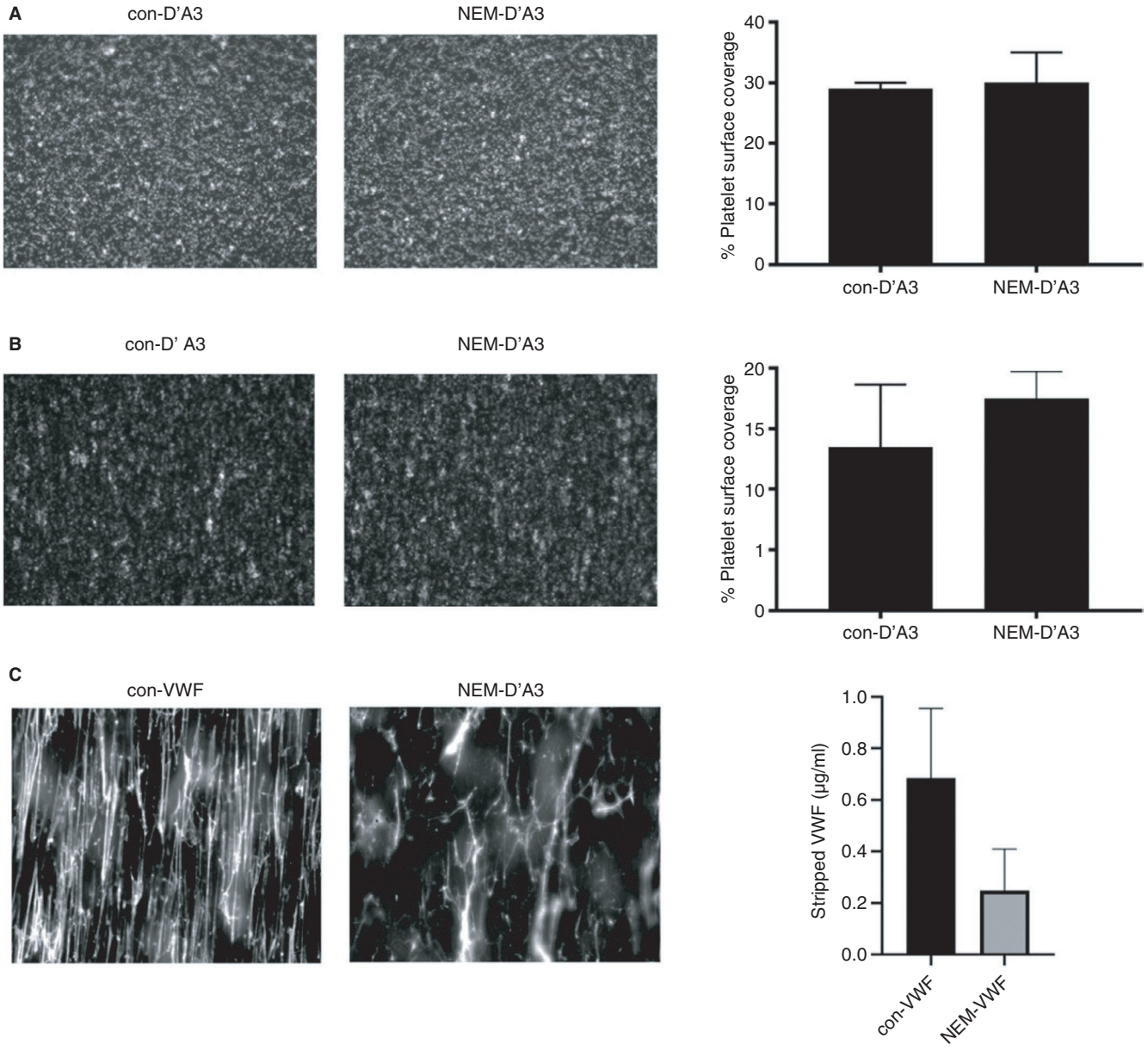

FIGURE 5 VWF thiols mediate collagen binding but not platelet binding. A, Ibidi VI$^{0.1}$ flow slides were coated with 40 µg/mL of either wild-type or NEM-treated VWFD′A3 and perfused with washed red blood cells and platelets at 1500 s^{-1}. B, Ibidi VI$^{0.1}$ flow slides coated with 100 µg/mL human collagen type III were incubated with 200 µg/mL of either wild-type or NEM-treated VWFD′A3 for 60 min at room temperature. After slides were washed, they were perfused with washed red blood cells and platelets. C, Custom made flow channels (100 µm high × 100 µm wide) were coated with 200 µg/mL collagen type I and perfused with 488-VWF at a final wall shear rate of 66 000 s^{-1} and images captured in real-time. D, Ibidi I$^{0.1}$ channel slides were coated with 200 µg/mL collagen type I and perfused with 10 µg/mL VWF in 20 mM Tris, pH 7.4 for 5 min. Following perfusion, bound protein was recovered by stripping with 2% sodium dodecyl sulfate at 60°C for 30 min. VWF concentration was determined by VWF ELISA. Data are mean ± SD (n = 3)

In keeping with previously published data, control VWF-488 formed a dense fiber network at 66 000 s^{-1} with the VWF fibers aligning in the direction of flow. In contrast, visibly fewer fibers were formed with NEM-VWF-488; fibers were more disjointed and not all fibers aligned in the direction of flow (Figure 5C). Similar results were obtained when non-Alex Fluor 488 labelled control and NEM-VWF were perfused over collagen at high shear and subsequently stained with anti-VWF-FITC antibodies (Figure S3B). Following perfusion with VWF, surfaces were also stripped and the amount of recovered VWF determined by ELISA. Compared with con-VWF, significantly less NEM-VWF was recovered from the flow chamber surface (Figure 5D). These data demonstrate that the reduced platelet capture observed with NEM-VWF is due to reduced ability of NEM-VWF to bind to collagen under high shear conditions and highlight a novel role for VWF free thiols in mediating collagen binding at high shear.

3.5 | Blocking VWF free thiols reduces the strength and life-time of the vwf-collagen bond

To directly detect alterations in the VWF-collagen binding interaction resulting from loss of free thiols, we used AFM to probe the collagen-VWF bond. The specificity of the VWF-collagen interaction was first validated by the significant decrease in adhesion frequencies when either collagen or VWF was absent and furthermore by significantly decreased adhesion to the W1745C collagen binding mutation (Figure 6A). We have previously demonstrated that this von Willebrand disease causing mutation ablates binding to collagen.[39] Figure 6B shows typical pulling traces without (upper) or with (lower) the rupture force of the collagen-VWF bond. The unbinding force of the collagen-VWF bond is derived from the force jump that accompanies the unbinding event. The unbinding forces were sorted and plotted as a dynamic force spectrum (Figure 6C); a plot of most probable unbinding force (Figure S4) as a function of the loading rate, and is a quantitation of the mechanical property of a ligand-receptor bond.[40] The unbinding force of con-VWF-collagen bond increased linearly with the logarithm of the loading rate, ranging from 37 to 95 pN over a loading rate of 400 to 6400 pN/s, respectively (Figure 6C). Compared with the con-VWF-collagen interaction, NEM-VWF showed significantly reduced unbinding forces under the six loading rates tested, indicating binding defects in NEM-VWF (Figure 6C). Fitting the Bell-Evans model to these data revealed that the con-VWF-collagen bond has a dissociate rate (ko)

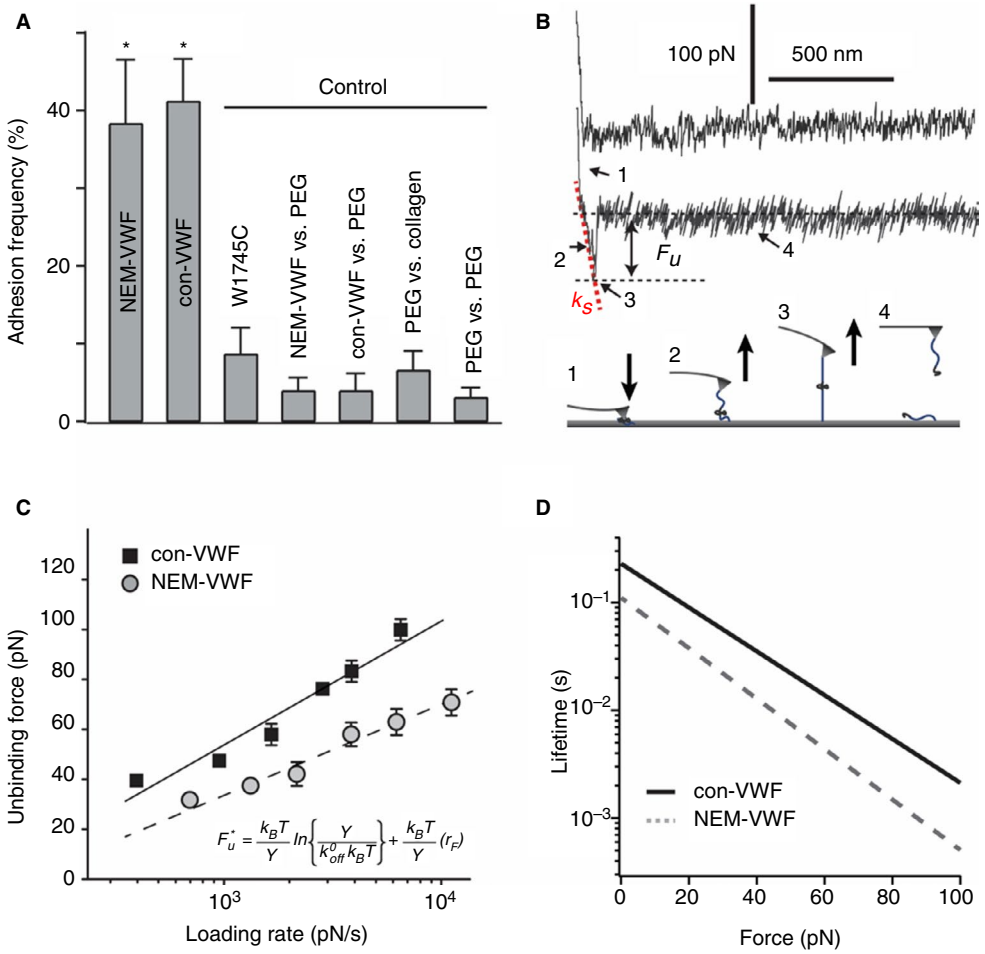

FIGURE 6 AFM measurement of VWF-collagen interaction. A, The adhesion frequency of the AFM measurements for different interacting pairs. Contact force, contact time, and retraction speed for all the interacting AFM tips and surfaces were set at 200 pN, 0.15 s, and 3.7 mm/s, respectively. The error bar is standard deviation with n = 5 (AFM cantilever) in each case. *Indicates $P < .001$ compared with any control groups. The *P* value was calculated by the Student *t* test. B, The upper panel shows two sample AFM pulling traces of the VWF-collagen interaction. The first (upper) trace had no interaction and the second (lower) trace shows the rupture force of a single conVWF-collagen complex. *Fu* is the unbinding force. *ks* is the system spring constant and was derived from the slope of the force-displacement trace. The lower panel illustrates the four stages of stretching and rupturing a single ligand-receptor complex using the AFM. C, The dynamic force spectra (ie, the plot of most probable unbinding force, *Fu*, as a function of loading rate, *rF*) of the VWF-collagen interactions. Unbinding forces at different loading rates were plotted as histograms (Figure S3). The peak of each histogram was plotted against the loading rate; uncertainty in force is shown as half bin-width. Some error bars are within the symbol. Equations to extract dissociate rate k^0 are shown. D, Comparison of bond lifetime as a function of the force of con-VWF-collagen and NEM-VWF collagen interactions. The force-dependent lifetimes (1/dissociation rate) of the bond were determined by $toff(f) = k0^{-1}\exp(-f/kBT)$, using the Bell-Evans' model parameters

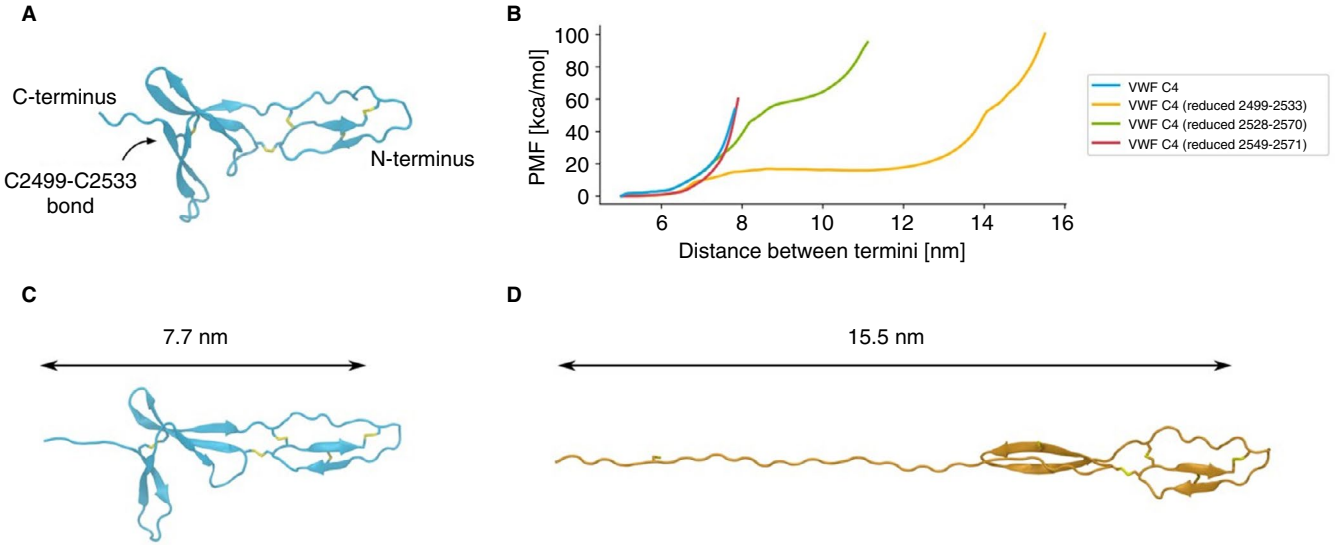

FIGURE 7 Molecular models of VWF stretching. We used molecular dynamics simulations to compute the forces required to pull apart the termini of a single C4 domain of VWF. A, Native structure of the VWF C4 domain (PDB code 6FWN). B, Potential mean force profile for pulling the termini apart in native VWF C4 and upon reduction of three different disulphide bonds. C, Structure of the stretched native VWF C4 with all disulphide bonds formed. D, Structure of the stretched VWF C4 domain after reduction of the 2499-2533 bond

of 4.3 ± 1.1 s^{-1}, whereas NEM-VWF yielded a ko of 9.0 ± 2.1 s^{-1} (Figure 6C). Figure 6D presents the force-dependent lifetime of the VWF-collagen interactions. Compared with con-VWF, NEM-VWF yielded an over 2-fold shorter lifetime at no force, and the lifetime of the NEM-VWF-collagen bond decreased more rapidly than con-VWF with increasing force. At 100 pN, the lifetime of NEM-VWF-collagen bond becomes 9-fold shorter than the conVWF-collagen bond. Because higher shear rate is associated with greater forces acting on the VWF-collagen bond, the AFM data can explain the effect of NEM treatment on VWF-collagen binding.

3.6 | Free thiols in the C-domains of VWF may affect domain flexibility

Our data suggest that under shear stress the bond between NEM-VWF and collagen either does not form or cannot respond normally to shear stress. Because this appears not to involve the formation of covalent interactions, we explored the possibility that free thiols increase the flexibility of the VWF C-domains. Using the recently described structure of the VWF C4 domain we performed molecular simulation on either the intact domain, or with the C2499-C2533 bond reduced, the C2528-C2570 bond reduced or the C2549-C2571 bond reduced, by applying a force to pull the domain from either terminus. The reduced cysteines have been previously demonstrated to be unpaired in some VWF molecules. We performed a PMF calculation to gain a quantitative insight into the differences in the energy required to stretch the domain in each case (Figure 7B). In the base state, the termini are 3.8 nm apart and during extension, more extension force is required as the distance between them becomes larger. Interestingly, the maximum extension reached with the nonreduced C4 domain is 7.7 nm, (Figure 7C); however, when the C2499-C2533 bond is reduced, less force is required to separate the termini and the domain can be further stretched to 15.5 nm (Figure 7D). These data suggest reduction of the disulphide bonds provides flexibility to the C-domains. In addition, the presence of free thiols in the structure opens the possibility of their exchange with other cysteines within the domain. In simulations using both C2499-C2533 and C2549-C2571 bonds reduced, the free thiol group from cysteine C2571 can become close enough to the C2528-C2570 bond to induce thiol exchange. Assuming this exchange takes place, the domain can further be stretched to 25.6 nm (Figure S5).

4 | DISCUSSION

Although previous studies have demonstrated a critical role for VWF free thiols, these have been performed using the plate and cone viscometer or the perfusion of soluble VWF over stimulated human umbilical vein endothelial cells, which does not consider the functional requirement for VWF to bind to collagen under shear during normal haemostasis.[8,11] The findings presented in this study demonstrate a previously unrecognized role for VWF free thiols in facilitating effective binding to collagen under conditions of high and pathological shear rates. Using an in vitro flow model, we demonstrate that blocking VWF free thiols reduces VWF-mediated platelet capture onto collagen in a shear-dependent manner, with almost no platelet capture occurring at 5000 s^{-1} and above. The effect is apparently not from altered platelet capture; NEM treatment of a VWF fragment encompassing the D′A3 domains had no effect on platelet capture potential and moreover, NEM-VWF was still able to mediate platelet binding to collagen between 500 and 1500 s^{-1}, where VWF is critical.[41] We could not fully exclude a potential role for the interaction with platelet GPIIbIIIa in this study. Because the

RGD sequence is located within the C-terminal domains, specifically within the C4 domain, blockade of free thiols anywhere in this region may affect GPIIbIIIa binding. Although we did not observe any differences in binding of NEM-VWF to GPIIbIIIa under static conditions, this may not be the case under conditions of high shear stress as we observed with collagen binding. Further studies will be needed to determine if thiol blockade affects the interaction of VWF with GPIIbIIIa at pathological flow rates. However, it has been previously shown that mutation of the RGD sequence does not affect the platelet capture function of VWF in flow assay systems and thus even if thiol blockade does modify the interaction of VWF with GPIIbIIIa, it would not be expected to significantly reduce or ablate platelet capture, as we observe. We therefore demonstrate that the reduction in platelet capture is due to reduced collagen binding by NEM-VWF which although normal under static conditions, becomes significantly reduced as the shear rate increases. This was confirmed by the direct visualization of VWF fibers formed under high pathological shear and quantification of bound VWF stripped from collagen surfaces. Interestingly, because these experiments were performed in the absence of plasma or platelets, the data also suggest that there is no specific requirement for an external thiol-reductase enzyme to modulate VWF thiols, although this cannot be fully excluded. Definitively, probing the VWF-collagen bond with AFM demonstrated that blocking VWF free thiols reduces the duration of the collagen bond lifetime and bond strength. The analysis shows that this effect is proportionately much greater at higher forces, representative of higher shear rates, which is consistent with the reduced binding under flow. VWF is known to undergo some conformational changes on binding to collagen and the loss of the biphasic binding after NEM treatment indicates a loss of structural flexibility.[42] Because high-affinity VWF binding to collagen requires multiple binding interactions between A3 domains and collagen (more so at high shear), the loss of structural flexibility is likely to be magnified under high shear stress conditions. It is not entirely clear how unpaired cysteine residues in the C-domains of VWF would alter the collagen binding function of the A3 domain or the availability of the A1 domain but these are clearly important effects. Ganderton et al suggested that lateral disulphide exchange involving C2431, C2453, C2451, and C2468 in the C3 domain occurs enabling cross-linking of VWF multimers. This would serve to enhance the network of VWF molecules binding to sites of injury, allowing the molecule to withstand the shear forces of the flowing blood and remain anchored to collagen. However, we previously failed to reproduce the findings of Ganderton et al[10] and some ambiguity exists regarding to the ability of soluble VWF to directly bind to immobilized VWF molecules under shear stress as has been previously suggested.[43]

Nonetheless, consistent with previous observation, we confirmed that VWF can assemble into ultra-large fibers that can be directly visualized under high pathological shear rates suggesting that some form of multimer–multimer interaction is occurring.[24,44-46] We therefore propose that following collagen binding under high shear, adjacent VWF multimers can associate in a thiol-independent manner as a consequence of their close proximity to each other after collagen binding, rather than as a result of a VWF-VWF capture mechanism.

To understand how free thiols largely located in the C domains might alter the ability of the required multiple A3 domains to bind to collagen, we examined their effect on the flexibility of the VWF molecule. To do this, we used the recently published structure of the C4 domain and performed molecular simulations pulling the molecule from both termini. Interestingly, when one of the disulphide pairs (C2499-C2533) is reduced, the VWF C4 domain model extends more readily in response to being "pulled" and the domain can be further stretched when two disulphide pairs are reduced. Although this is only a single C-domain and does not represent a collagen bound VWF multimer, it is nonetheless suggestive that free thiols in the C-domains offer a degree of flexibility to the VWF molecule that would potentially enable a VWF multimer to withstand the shear stress imparted to it during and after collagen binding. Such elongation may bring free thiols into proximity with intact disulphide bonds allowing disulphide exchange.[47,48] We modelled the potential reshuffling of disulphides at two different positions, showing that it increases the ability of the VWF C4 domain to extend under shear stress. From these data, disulphide exchange is likely to be within individual VWF multimers: although we cannot exclude that a free thiol from one multimer reduces a disulphide bond in another multimer, our data do not support the notion of covalent cross-linking between multimers; however, further work is required to investigate this. Following blockade with NEM, the initial free thiols are not present and therefore spontaneous disulphide rearrangement cannot occur following collagen binding. As such, the C-terminus of VWF is less flexible and is unable to withstand high shear forces causing the VWF-collagen bond to rupture. Under lower shear rates, the forces generated on the collagen bound molecule are not significant enough to break the bond and free thiol exchange is not required. Further work is now required to fully understand this process. Nonetheless, although the exact mechanism requires defining, the effect of blocking VWF free thiols has the most significant effect at very high and, importantly, pathological shear rates and thus represents a way to modulate VWF function specifically under pathological conditions without affecting the function of VWF in normal hemostasis. In conclusion, our data demonstrate a previously unrecognized role for VWF free thiols in mediating collagen binding at high shear rates and targeting VWF thiols may be a novel and safe antithrombotic strategy.

ACKNOWLEDGMENTS

T.A.J. McKinnon was supported by a British Heart Foundation Basic Science Intermediate Fellowship Grant (FS/11/3/28632). We are grateful for support from Imperial College BRC.

CONFLICT OF INTEREST

The authors state they have no conflict of interest.

AUTHOR CONTRIBUTIONS

Harrison E.R. O'Brien performed experiments and analyzed data; X. Frank Zhang designed and performed experiments and wrote the paper; Maximo Sanz-Hernandez designed and performed

experiments, analyzed data, and wrote the paper; Susan Shapiro performed experiments; Golzar Mobayen performed experiments; Yan Xu performed experiments; Alfonso De Simone designed experiments; Michael A. Laffan designed the study and wrote the paper; and Thomas A.J. McKinnon designed the study, performed experiments, analyzed data, and wrote the paper.

REFERENCES

1. Sadler JE. Biochemistry and genetics of von Willebrand factor. *Annu Rev Biochem*. 1998;67:395-424.
2. Nogami K, Shima M, Nishiya K, et al. A novel mechanism of factor VIII protection by von Willebrand factor from activated protein C-catalyzed inactivation. *Blood*. 2002;99(11):3993-3998.
3. Miseta A, Csutora P. Relationship between the occurrence of cysteine in proteins and the complexity of organisms. *Mol Biol Evol*. 2000;17(8):1232-1239.
4. Wagner DD, Marder VJ. Biosynthesis of von Willebrand protein by human endothelial cells: processing steps and their intracellular localization. *J Cell Biol*. 1984;99(6):2123-2130.
5. Xie L, Chesterman CN, Hogg PJ. Reduction of von Willebrand factor by endothelial cells. *Thromb Haemost*. 2000;84(3):506-513.
6. Ganderton T, Berndt MC, Chesterman CN, Hogg PJ. Hypothesis for control of von Willebrand factor multimer size by intra-molecular thiol-disulphide exchange. *J Thromb Haemost*. 2007;5(1):204-206.
7. Marti T, Rosselet SJ, Titani K, Walsh KA. Identification of disulfide-bridged substructures within human von Willebrand factor. *Biochemistry*. 1987;26(25):8099-8109.
8. Choi H, Aboulfatova K, Pownall HJ, Cook R, Dong JF. Shear-induced disulfide bond formation regulates adhesion activity of von Willebrand factor. *J Biol Chem*. 2007;282(49):35604-35611.
9. Ganderton T, Wong JW, Schroeder C, Hogg PJ. Lateral self-association of VWF involves the Cys2431-Cys2453 disulfide/dithiol in the C2 domain. *Blood*. 2011;118(19):5312-5318.
10. Shapiro SE, Nowak AA, Wooding C, Birdsey G, Laffan MA, McKinnon TA. The von Willebrand factor predicted unpaired cysteines are essential for secretion. *J Thromb Haemost*. 2014;12(2):246-254.
11. Li Y, Choi H, Zhou Z, et al. Covalent regulation of ULVWF string formation and elongation on endothelial cells under flow conditions. *J Thromb Haemost*. 2008;6(7):1135-1143.
12. Zhou YF, Eng ET, Nishida N, Lu C, Walz T, Springer TA. A pH-regulated dimeric bouquet in the structure of von Willebrand factor. *EMBO J*. 2011;30(19):4098-4111.
13. Zhou YF, Eng ET, Zhu J, Lu C, Walz T, Springer TA. Sequence and structure relationships within von Willebrand factor. *Blood*. 2012;120(2):449-458.
14. Muller JP, Lof A, Mielke S, et al. pH-dependent interactions in dimers govern the mechanics and structure of von Willebrand factor. *Biophys J*. 2016;111(2):312-322.
15. Muller JP, Mielke S, Lof A, et al. Force sensing by the vascular protein von Willebrand factor is tuned by a strong intermonomer interaction. *Proc Natl Acad Sci U S A*. 2016;113(5):1208-1213.
16. Bark DL Jr, Ku DN. Wall shear over high degree stenoses pertinent to atherothrombosis. *J Biomech*. 2010;43(15):2970-2977.
17. Li MX, Beech-Brandt JJ, John LR, Hoskins PR, Easson WJ. Numerical analysis of pulsatile blood flow and vessel wall mechanics in different degrees of stenoses. *J Biomech*. 2007;40(16):3715-3724.
18. Banerjee RK, Back LH, Back MR, Cho YI. Physiological flow analysis in significant human coronary artery stenoses. *Biorheology*. 2003;40(4):451-476.
19. Fuchs B, Budde U, Schulz A, Kessler CM, Fisseau C, Kannicht C. Flow-based measurements of von Willebrand factor (VWF) function: binding to collagen and platelet adhesion under physiological shear rate. *Thromb Res*. 2010;125(3):239-245.
20. O'Donnell JS, McKinnon TA, Crawley JT, Lane DA, Laffan MA. Bombay phenotype is associated with reduced plasma-VWF levels and an increased susceptibility to ADAMTS13 proteolysis. *Blood*. 2005;106(6):1988-1991.
21. Nowak AA, Canis K, Riddell A, Laffan MA, McKinnon TA. O-linked glycosylation of von Willebrand factor modulates the interaction with platelet receptor glycoprotein Ib under static and shear stress conditions. *Blood*. 2012;120(1):214-222.
22. Fu H, Jiang Y, Yang D, Scheiflinger F, Wong WP, Springer TA. Flow-induced elongation of von Willebrand factor precedes tension-dependent activation. *Nat Commun*. 2017;8(1):324.
23. Lankhof H, Wu YP, Vink T, et al. Role of the glycoprotein Ib-binding A1 repeat and the RGD sequence in platelet adhesion to human recombinant von Willebrand factor. *Blood*. 1995;86(3):1035-1042.
24. Colace TV, Diamond SL. Direct observation of von Willebrand factor elongation and fiber formation on collagen during acute whole blood exposure to pathological flow. *Arterioscler Thromb Vasc Biol*. 2013;33(1):105-113.
25. Ebner A, Wildling L, Kamruzzahan AS, et al. A new, simple method for linking of antibodies to atomic force microscopy tips. *Bioconjug Chem*. 2007;18(4):1176-1184.
26. Zhang X, Craig SE, Kirby H, Humphries MJ, Moy VT. Molecular basis for the dynamic strength of the integrin alpha4beta1/VCAM-1 interaction. *Biophys J*. 2004;87(5):3470-3478.
27. Fu X, Xu Y, Wu C, Moy VT, Zhang X. Anchorage-dependent binding of integrin I-domain to adhesion ligands. *J Mol Recognit*. 2015;28(6):385-392.
28. Zhang X, Wojcikiewicz E, Moy VT. Force spectroscopy of the leukocyte function-associated antigen-1/intercellular adhesion molecule-1 interaction. *Biophys J*. 2002;83(4):2270-2279.
29. Jorgensen WLCJ, Madura JD, Impey RW, Klein ML. Comparison of simple potential functions for simulating liquid water. *J Chem Phys*. 1983;79(2):926.
30. Bussi G, Donadio D, Parrinello M. Canonical sampling through velocity rescaling. *J Chem Phys*. 2007;126(1):014101.
31. Berendsen HJCPJ, van Gusteren WF, DiNola HJR. Molecular dynamics with coupling to an external bath. *J Chem Phys*. 1984;81(8):3684-3690.
32. Hess BBH, Berendsen HJC, Fraaije JGE. MLINCS: a linear constraint solver for molecular simulations. *J Comput Chem*. 1997;18(12):1463-1472.
33. Darden TYD, Pedersen L. Particle mesh Ewald: an N log(N) method for Ewald sums in large systems. *J Chem Phys*. 1993;98(12):10089.
34. Lindorff-Larsen K, Piana S, Palmo K, et al. Improved side-chain torsion potentials for the Amber ff99SB protein force field. *Proteins*. 2010;78(8):1950-1958.
35. Roux B The calculation of the potential of mean force using computer simulations. *Comput Phys Commun*. 1995;91(1-3):275-282.
36. Pronk S, Pall S, Schulz R, et al. GROMACS 4.5: a high-throughput and highly parallel open source molecular simulation toolkit. *Bioinformatics*. 2013;29(7):845-854.
37. McKinnon TA, Goode EC, Birdsey GM, et al. Specific N-linked glycosylation sites modulate synthesis and secretion of von Willebrand factor. *Blood*. 2010;116(4):640–648.
38. Nowak AA, McKinnon TA, Hughes JM, Chion AC, Laffan MA. The O-linked glycans of human von Willebrand factor modulate its interaction with ADAMTS-13. *J Thromb Haemost*. 2014;12(1):54-61.
39. Riddell AF, Gomez K, Millar CM, et al. Characterization of W1745C and S1783A: 2 novel mutations causing defective collagen binding in the A3 domain of von Willebrand factor. *Blood*. 2009;114(16):3489-3496.
40. Evans E. Probing the relation between force–lifetime–and chemistry in single molecular bonds. *Annu Rev Biophys Biomol Struct*. 2001;30:105-128.
41. Ruggeri ZM. Structure of von Willebrand factor and its function in platelet adhesion and thrombus formation. *Best Pract Res Clin Haematol*. 2001;14(2):257-279.

42. Bendetowicz AV, Wise RJ, Gilbert GE. Collagen-bound von Willebrand factor has reduced affinity for factor VIII. *J Biol Chem*. 1999;274(18):12300-12307.
43. Savage B, Sixma JJ, Ruggeri ZM. Functional self-association of von Willebrand factor during platelet adhesion under flow. *Proc Natl Acad Sci U S A*. 2002;99(1):425-430.
44. Zheng Y, Chen J, Lopez JA. Flow-driven assembly of VWF fibres and webs in in vitro microvessels. *Nat Commun*. 2015;6:7858.
45. Barg A, Ossig R, Goerge T, et al. Soluble plasma-derived von Willebrand factor assembles to a haemostatically active filamentous network. *Thromb Haemost*. 2007;97(4):514-526.
46. Schneider SW, Nuschele S, Wixforth A, et al. Shear-induced unfolding triggers adhesion of von Willebrand factor fibers. *Proc Natl Acad Sci U S A*. 2007;104(19):7899-7903.
47. Kolsek K, Aponte-Santamaria C, Grater F. Accessibility explains preferred thiol-disulfide isomerization in a protein domain. *Sci Rep*. 2017;7(1):9858.
48. Levin L, Zelzion E, Nachliel E, Gutman M, Tsfadia Y, Einav Y. A single disulfide bond disruption in the beta3 integrin subunit promotes thiol/disulfide exchange, a molecular dynamics study. *PLoS One*. 2013;8(3):e59175.

SUPPORTING INFORMATION

Additional supporting information may be found online in the Supporting Information section.

How to cite this article: O'Brien HER, Zhang XF, Sanz-Hernandez M, et al. Blocking von Willebrand factor free thiols inhibits binding to collagen under high and pathological shear stress. *J Thromb Haemost*. 2021;19:358–369. https://doi.org/10.1111/jth.15142